

Lungs X-Ray Image Segmentation and Classification of Lung Disease Using Convolutional Neural Network Architectures

Bambang Suprihatin , Yuli Andriani , Fauziah Nuraini Kurdi , Anita Desiani , Ibra Giovani Dwi Putra , Muhammad Akmal Shidqi
Universitas Sriwijaya, Indralaya, Indonesia

Article Info

Article history:

Received July 09, 2023
Revised September 14, 2023
Accepted September 29, 2023

Keywords:

Classification
Convolutional Neural Network
Lung Disease
Segmentation

ABSTRACT

Lung disease is one of the biggest causes of death in the world. The SARS-CoV-2 virus causes diseases like COVID-19, and the bacteria Streptococcus sp., which causes pneumonia, are two sample causes of lung disease. X-ray images are used to detect the lung disease. This study aimed to combine the stages of segmentation and classification of lung disease. This study in segmentation aims to separate the features contained in the lung images. The classification aimed to provide holistic information on lung disease. This research method used the Deep Residual U-Net (DrU-Net) segmentation architecture and the Deep Residual Neural Network (DResNet) classification architecture. DrU-Net is a modified U-Net architecture with dropout added in its convolutional layers. DResNet is a modified Residual Network (ResNet) architecture with dropout added in its convolutional block layers. The result of this study was segmentation using the DrU-Net architecture obtained 99% for accuracy, 98% for precision, 98% for recalls, 98% for F1-Score, and 96.1% for IoU. The classification results of the segmented images using the DResNet architecture obtained 91% for accuracy, 86% for precision, 85% for recalls, and 84% for F1-Score. The performance results of DrU-Net architecture were excellent and robust in image segmentation. Unfortunately, the average performance of DResNet in classification was still below 90%. These results indicate that Dres-Net performs well in classifying lung disorders in 3 labels, namely Covid, Normal, and Pneumonia, but still needs improvement.

Copyright ©2022 The Authors.
This is an open access article under the [CC BY-SA](#) license.



Corresponding Author:

Anita Desiani,
Mathematics Departement,
Universitas Sriwijaya, Indralaya, Indonesia,
Email: anita_desiani@unsri.ac.id

How to Cite:

B. Suprihatin, Y. Andriani, F. Kurdi, A. Desiani, I. Dwi Putra, and M. Shidqi, "Lungs X-Ray Image Segmentation and Classification of Lung Disease Using Convolutional Neural Network Architectures", *MATRIK: Jurnal Manajemen, Teknik Informatika, dan Rekayasa Komputer*, Vol. 23, No. 1, pp. 67-78, Nov, 2023.

This is an open access article under the CC BY-SA license (<https://creativecommons.org/licenses/by-sa/4.0/>)

1. INTRODUCTION

Lung disease is one of the leading causes of death for men and the third biggest cause of death for women after breast and colorectal cancer [1]. The lungs have a main function that performs well in classifying lung disorders into three labels, namely Covid, Normal, and Pneumonia, but still needs improvement; where there is an exchange of oxygen and carbon dioxide, excess carbon dioxide will stimulate the respiratory center and increase the inspiratory and expiratory signals to the respiratory muscles [2]. If lung function is impaired, the health of the entire human body can be greatly affected. Viruses and bacteria are two causes of lung disease. Viruses are the most common cause of acute respiratory infections, and the causative agents of lower respiratory tract infections depend on the patient's age and immunity [3]. The current worldwide virus is the Severe Acute Respiratory Syndrome Corona Virus 2, which can be shortened to SARS-CoV-2. According to WHO, on May 11, 2022, the number of sufferers was 514,948,748 confirmed worldwide, and 6,253,507 sufferers died caused by the virus or as much as 1.2% of the total sufferers of COVID-19 [4]. Apart from viruses, pneumonia is a common disease. Pneumonia is a condition in which an infection occurs in the air sacs in the person's lungs. Pneumonia occupies a very large burden of disease worldwide, exceeding diseases such as cancer, diabetes, HIV/AIDS, malaria, and many other diseases recognized as major health problems worldwide [5].

X-ray images can be used as one method of lung disease detection. Segmentation techniques are required to observe the lungs on X-ray images. Segmentation can be categorized into two categories: manual segmentation and automatic segmentation. The manual segmentation performed on X-ray images to obtain lung features requires experts, a lot of time, expensive costs, and subjective assessment [6]. Another technique to overcome the limitations of manual segmentation is automatic segmentation. Automatic segmentation offers several advantages, such as faster time and rapid outcomes without human involvement. The consistency of automated results reduces errors caused by human judgment. Automatic segmentation can handle a huge amount of image segmentation data. One of the methods used for processing images in automatic segmentation is CNN (Convolutional Neural Network) [7]. The utilization of CNN in image segmentation has been widely developed in various studies. Humera and Kattula applied CNN U-Net for lung image segmentation, but their results, accuracy, precision, and recall of the study were below 90% [8]. Xiaorui et al. used AE-CNN for lung image segmentation, but their performance results were still below 85%, and their results showed 93.17% accuracy, 93.57% recall, and 93.12% F1-Score [9]. Aslan et al. used R-CNN for lung image segmentation; the accuracy, precision, and recall are 95% [10]. U-Net is the popular architecture in segmentation. Some advantages of U-Net are its effectiveness in handling image segmentation tasks, the ability to capture both local and global features through its U-shaped architecture, and its suitability for tasks with limited data. Anupam used U-Net for lung segmentation, and their results showed 97.09% accuracy, 95.73% sensitivity, and 97.55% F1-Score [11]. Muhammet used U-Net for lung segmentation, and their performance results are excellent, above 95% [12]. Niranjana et al. also used U-Net for lung segmentation; their results were excellent [13]. However, these studies concentrated only on segmentation images. Segmentation only provides information about specific features an expert gives, but it does not offer a holistic understanding of a lung. Classification is required to provide holistic information labeling to obtain a comprehensive label of a condition's information. Segmentation typically offers information for experts to determine the condition of a lung, while classification provides information that patients or the public can understand regarding the presence of a lung disorder [14].

The implementation of segmentation can enhance classification performance. It can overcome detection issues that specifically pertain to lung-related areas. Segmentation is a crucial component in classification as it aids in improving classification performance. CNN architecture has many architectures in classification. One of the CNN architectures for classification is ResNet. ResNet's advantages are handling deeper networks without decreasing performance due to skipping connections and overcoming the problem of loss of gradients by leftover blocks, thus overcoming the problem of loss of gradients [15]. The ResNet architecture also facilitates the training of very deep neural networks, enabling better feature extraction and representation, ultimately leading to improved classification accuracy [16]. Subrato et al. applied ResNet for lung classification. The results of the accuracy and F1-Score of the study are more than 90%, but the sensitivity was only 83.5% [17]. Talibi et al. used ResNet for lung classification, and their sensitivity and F1-Score were only 78.73% and 76.80% [18]. Yi et al. used ResNet for lung classification, but their results were very bad, below 60% [19]. These studies have not involved the segmentation stage in classifying lung disease disorders. However, ResNet has several limitations, such as the deeper architecture's higher complexity and computational cost. The limitation can consume much time for training and require more resources.

Although U-Net and ResNet are popular CNN architectures in image processing, they are known as deep architectures, resulting in a large number of parameters. The large number of parameters can lead to overfitting. One technique to overcome overfitting is dropout. Dropout is a technique in machine learning and artificial neural networks. During training, some units (neurons) in dropout are randomly excluded or "dropped out" from the network with a certain probability [20]. Dropout helps prevent overfitting by reducing the reliance on specific individual units in the network during training. Li et al. used dropout in ResNet architecture for heart arrhythmia disease classification. The accuracy, specificity, and F1-Score were above 90%, but the sensitivity was only 84.5% [21]. Ali and Mallaiah used dropout in CNN-SVM architecture for handwritten classification. The study obtained excellent accuracy,

sensitivity, specificity, and F1-Score results above 90% [22]. Milans et al. used dropout in DenseNet architecture for epilepsy disease classification with 92.48% accuracy, 92.15% sensitivity, 91.14% specificity, and 92.31% F1-Score [23]. Unfortunately, these studies also did not involve the segmentation stage yet.

The novelty of this study is that it combines the segmentation and classification stages with CNN architecture. Unlike other studies that only focused on one stage (only segmentation or classification stage), this study focuses on two stages: segmentation and classification. For the segmentation stage of the study, DrU-Net architecture will be used. DrU-Net is a modified U-Net architecture with dropout added in its convolutional layers. This modification aims to reduce the complexity of U-Net and avoid an excessive growth in parameters. DResNet will be used for the classification stage in the study. DResNet architecture is a modified ResNet architecture with dropout added in its convolutional block layers. This modification aims to reduce the complexity of ResNet in dealing with excessive parameter growth. The input for the classification stage is the output obtained from the segmented image. The addition of dropout in both architectures is an effort to prevent the occurrence of overfitting. This study measured the performance based on the results of each architectural evaluation performance. Measurements for segmentation will involve accuracy, precision, recall, F1-Score, and IoU. The IoU is to measure the overlap between the predicted and actual segmentation masks to assess how well the predicted region aligns with the ground truth region. Classification measurement performances will involve accuracy, precision, recall, and F1-Score. The classification of lung disorders is grouped into three labels: Covid, Normal, and Pneumonia. This study combines the stages of segmentation and classification of lung disease. So, the contributions of this study can be used as an alternative architecture for the segmentation and classification of lung disease medical images. The paper in this study is divided into several sections. Section 1 is an introduction that presents the background of this study. Section 2 is a research method that presents the study's stages. Section 3 is results and analysis, which presents the results of the research method applied and compares the study results with other studies. Section 4 is the conclusion that presents the important points of the analysis carried out on the results obtained in Section 3.

2. RESEARCH METHOD

This study will combine the segmentation and classification processes to perform an image-based early detection of lung disease. The stages of segmentation and classification using CNN are depicted in a diagram. The diagram can be seen in Figure 1. In Figure 1, the segmentation and classification process begins with the input of the image, followed by the enhanced image by the CLAHE image. Then, proceed with segmentation using the DrU-Net architecture and classification using the DResNet architecture. After performing the segmentation and classification stages, the output results are graphics, accuracy, precision, recall, F1-Score, and ROC.

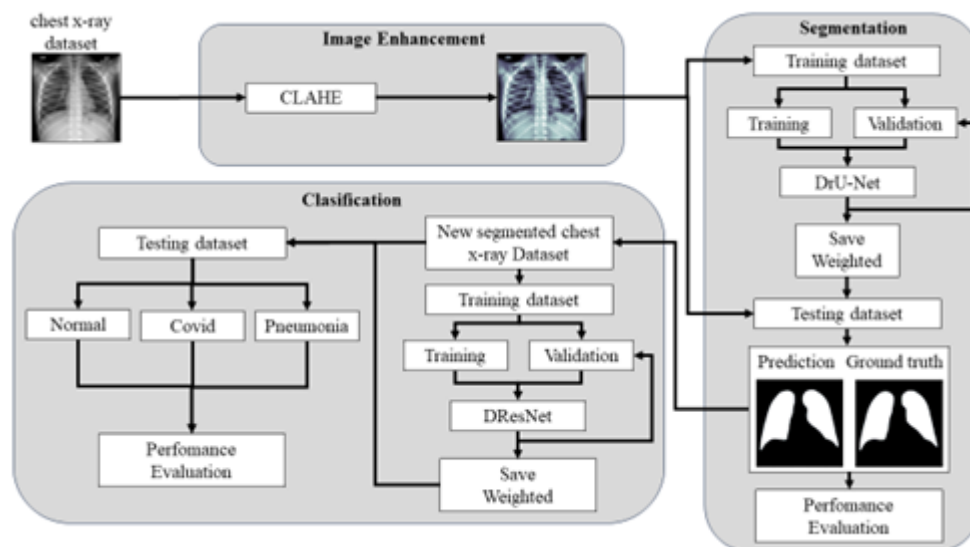


Figure 1. Diagram of the Stages of Segmentation and Classification of Lung Disease

2.1. Data Collection

The dataset used was taken from Kaggle, which was uploaded by Tawsifur Rahman, Dr. Muhammad Chowdhury, and Amith Khandakar in the form of X-ray results of the chest and masking of the lungsdataset obtained from <https://www.kaggle.com/datasets/tawsifurrahman/covid19-radiography-database>. The dataset consists of images with an average size of 299 x 299 pixels. Each image is classified into three classes, namely Covid, Normal, and Pneumonia. This study uses 504 images from each class, so the total images used are 1,512. X-Ray images have different resolutions, so the data size is converted to 256 x 256 pixels in the pre-processing stage.

2.2. Image Enhancement

Contrast Limited Adaptive Histogram Equalization (CLAHE) is used to increase the contrast of an image and overcome uneven colors. The initial step of CLAHE is to change the image to grayscale. After getting the value from the grayscale, the equation is used to calculate CLAHE using Equation (1). where I is the result of the CLAHE value; a is the number of pixels contained in each block, b is the dynamic range value in the block, α is the clip factor value, and S_{max} is the maximum slope value.

$$I = \frac{a}{b} \left(1 + \frac{\alpha}{100} (S_{max} - 1) \right) \quad (1)$$

2.3. Segmentation

512 images consisted of 3 classes, namely Covid, Normal and Pneumonia. The number of images in the Covid class is 504, the Normal class is 504, and the Pneumonia class is 504. The data is split by 80% for training and 20% for testing. The data will be used for segmentation using DrU-Net. The DrU-Net architecture can be seen in Figure 2.

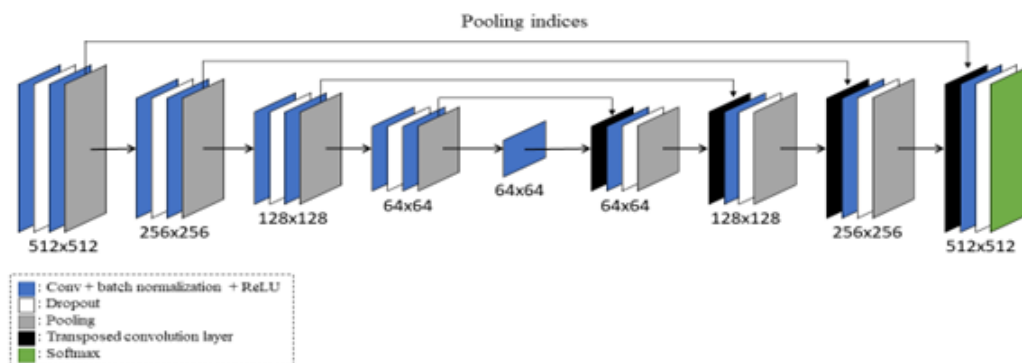


Figure 2. Architecture of DrU-Net

DrU-Net architecture in Figure 2 illustrates the training process at the segmentation stage. In this approach, the DrU-Net architecture on CNN is divided into two groups: the left side (encoder) and the right part (decoder). The encoder section consists of 4 layers where each layer has 2 convolution layers, 2 batch normalization layers, 1 grouping layer, and 1 spatial suppression layer. The step size in the convolution layer is 2. In the pooled layer, the maximum is used with 2x2. The convolutional filter layers in each block are 64, 128, 256, and 512. This function aims to apply thresholding to the pixel values in the input image. It sets a threshold value of 0, resulting in any pixel values below zero being set to 0.

1. Convolution Layer

The convolution layer is a fundamental building block in CNN used for tasks like image and video recognition. The convolution operation in a convolution layer involves sliding a set of filters (also known as kernels) over the input data and computing the element-wise dot product between the filter and the overlapping region of the input. This operation helps capture local patterns and features in the data [24]. The convolution layer function is defined in Equation (2). Where I_m is the input image. x and y are the coordinates of the top-left corner of the input image, F is the filter, k is the filter size. i and j are the filter's spatial indices.

$$C = \sum_{i=1}^k \sum_{j=1}^k Im(x + i, y + j) F(i, j) \tag{2}$$

2. ReLU

ReLU is an activation function commonly used in neural networks to introduce non-linearity to models. This is a simple but effective way to enable neural networks to learn complex relationships in data [20]. The ReLU activation function is defined in Equation (3), where R is the output of ReLU, while C is the result from the Convolution layer.

$$R = max(0, C) \tag{3}$$

3. Dropout

Dropout is a technique used to improve the performance and generalization of deep neural networks by preventing overfitting. The dropout is applied by randomly setting a portion of the inputs to zero during training. Dropout reduces the network’s capacity and compels the model to learn more reliable features that can work well even when some inputs are missing [20].

4. Softmax

The softmax activation function is employed in the output or final layer, particularly for binary classification, as it ensures a range of values between 0 and 1. The softmax activation function is defined in Equation (4). Where r is the input from ReLU, n is the number of samples, and e is Euler’s number irrational number approximately equal to 2.71828.

$$s(r)_i = \frac{e^{r_i}}{\sum_{j=0}^n e^{r_j}} \tag{4}$$

5. Classification

The CNN architecture is generally divided into 2, namely feature detection and classification layers. The feature detection layer changes the image to a number and then calculates the matrix. The feature detection layer displays operations on input data, including the convolutional layer, pooling layer, and rectified linear unit (ReLU), which will continue to repeat with each layer learning to get different results. One of the architectures contained in CNN is DResNet. DResNet is a modified ResNet architecture with dropout added in its convolutional block layers. The DresNet architecture can be seen in Figure 3.

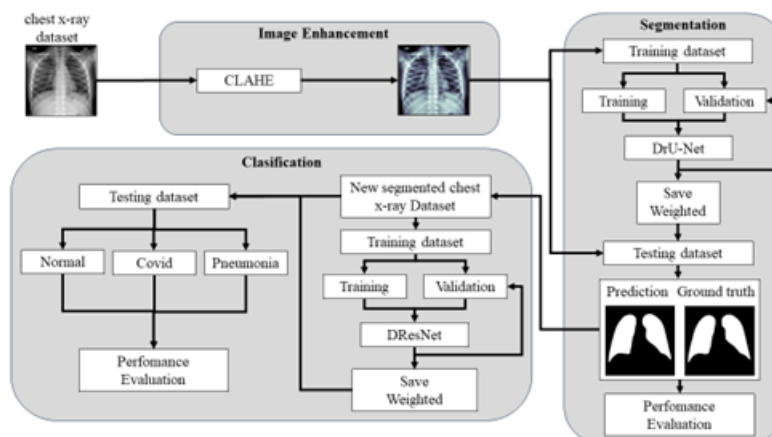


Figure 3. Architecture of DResNet

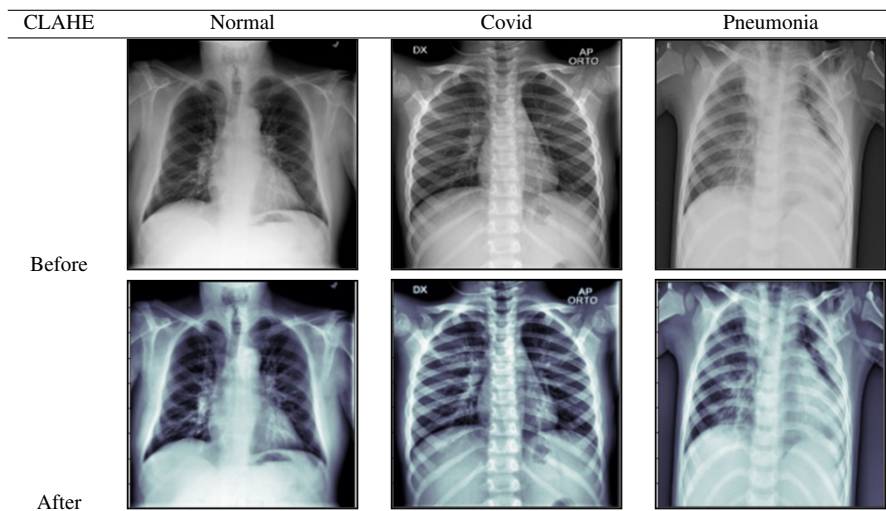
DResNet architecture in Figure 3 illustrates the training process at the classification stage. DResNet has a shortcut connection concept that prevents the system from losing a lot of information during training [25]. The input layer consists of the first convolution layer with the block of 7x7 kernel and 64 filter, dropout, and max-pooling of 3x3 kernel. The second layer consists of a convolution layer block of 1x1 kernel and 64 filter, 3x3 kernel and 64 filter, 1x1 kernel, and 256 filter, and ends with dropout. The third layer consists of a convolution layer block of 1x1 kernel and 128 filter, 3x3 kernel and 128 filter, 1x1 kernel, and 512 filter, and ends with dropout. The fourth convolution layer consists of a block of 1x1 kernel and 256 filter, 3x3 kernel and 256 filter, 1x1 kernel and 1024 filter, and ends with dropout. Then, it goes into the fifth convolution layer block of the 1x1 kernel and 512 filters, the 3x3 kernel and 512 filters, the 1x1 kernel and 2048 filter, and ends with a dropout. The final stage consists of average pooling, fully connected with 1000 filters and Softmax activation function.

3. RESULT AND ANALYSIS

3.1. Image Enhancement

In this study, the images were obtained from lung disease datasets regarding COVID-19 and Pneumonia. The original image in the dataset is a binary image. Since the dataset's image is not visible, CLAHE will be applied to it to make it more visible. A comparison of the original image with the CLAHE image can be seen in Table 1. In Table 1, it can be seen that there is a significant difference between the original image and the CLAHE. The image obtained after CLAHE has a better image than the original image from the dataset. After the image is enlarged in contrast with CLAHE and the results are good, the segmentation that will be carried out can obtain better results.

Table 1. Comparison Before and After CLAHE



3.2. Segmentation

In segmentation, the CNN method is applied with the DrU-NET architecture. This segmentation process was carried out using 1512 X-ray images enhanced with CLAHE. The graph regarding the accuracy and loss of the segmentation training results can be seen in Figure 4. Based on Figure 4, the performance results obtained from the segmentation results are excellent. After the accuracy reaches 0.98, the graph results become stable. While the loss becomes smaller, the graphics become more stable when it reaches the 5th epoch. It is found that the value of the accuracy and loss results using the segmentation results is said to be good from the training using the 40 epochs that were carried out. The excellent segmentation results mean that the machine learning of lung disease is working well. The weights of the training results model will be used in the testing process. The comparison of the results from segmentation using DrU-Net on testing with ground truth can be seen in Table 2.

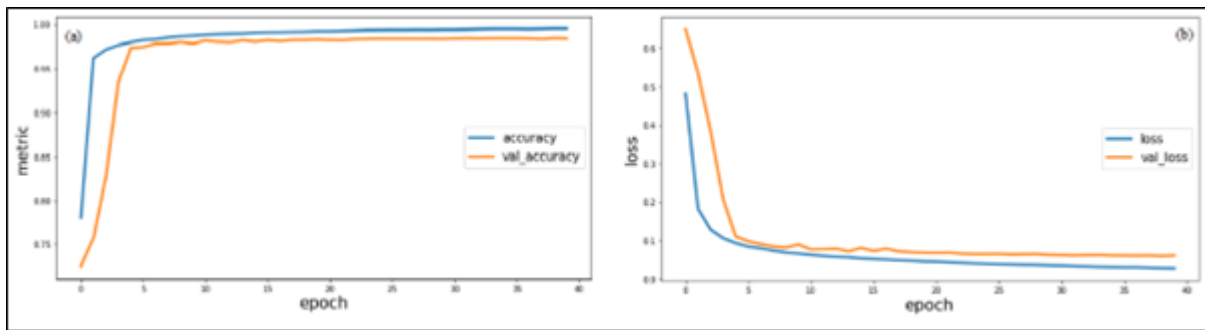


Figure 4. The Performance of DrU-Net on Graph (a) Accuracy (b) Loss

Table 2. Comparison of Segmentation Results using DrU-Net with Ground Truth

Name	Original Image	Segmentation	
		Ground Truth	Results
Test.01. jpg			
Test.02. jpg			
Test.03. jpg			

Based on the comparison between the segmentation results and the ground truth presented in Table 2, several metrics are employed to evaluate the performance of CNN segmentation using the DrU-NET architecture. These metrics include accuracy, precision/sensitivity, recall, F1-Score, specificity, and mean IoU. The segmentation results obtained an accuracy of 99%, a precision of 98%, a recall of 98%, an F1-Score of 98%, and a specificity of 97%. In addition to getting these values, a Mean IoU of 96% was obtained. With the segmentation results obtained, the performance graph of the segmentation model within all segmentation boundaries can be seen on the ROC graph, which can be seen in Figure 5.

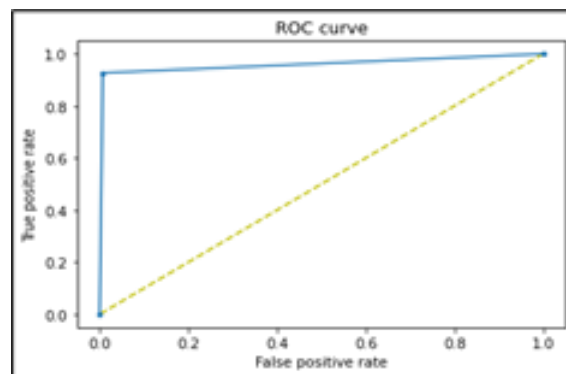


Figure 5. The Performance of Segmentation Results Using DrU-Net on The ROC Graph

Based on Figure 5, The results show that DrU-Net has an AUC of 0.93, which is excellent for lung segmentation on X-ray images. The excellent segmentation results mean that the machine learning of lung disease is working well. The values obtained from the segmentation results will be compared with the values obtained using other methods by previous studies. A comparison of the segmentation results of each method can be seen in Table 3.

Table 3. Comparison of Segmentation Methods

Method	Results				
	Accuracy (%)	Precision (%)	Recalls (%)	F1-Score (%)	Mean IoU (%)
Textures and Wavelet Features + SVM [14]	98.35	-	97.4	-	-
3DCC + CAM [26]	65.7	-	-	-	-
Anam-Net [27]	98.8	91.8	-	79.8	-
UNet [28]	96.6	50.6	98.3	40.1	29.1
Proposed Method	99	98	98	98	96

Based on Table 3, it shows that the research by [14] obtained excellent accuracy, but this study did not calculate recall, F1-Score, or mean IoU. Recall and f1-score can show the model's positive prediction ratio. Mean IoU is also rarely used by other researchers, even though we can find out how similar our segmented images are to the ground truth using mean IoU. After getting the results of the lung segmentation, a classification process will be carried out to determine the accuracy of the computer for classifying lung diseases. The research by [27] also shows excellent accuracy. However, the research got a f1-score under 80%, which shows that the model still struggles to detect the part needed in segmentation. The research by [28] also shows excellent accuracy. However, this study's precision, f1-score, and mean IoU are still very low, which shows that the model cannot be said to be excellent.

3.3. Classification

This classification uses the CNN method with the DResNet architecture. The classification process is carried out on 1,512 X-ray images, which have been grouped into three classes, namely Covid, Normal, and Pneumonia, with as many as 514 images for each class. The graph regarding the accuracy and loss of classification using segmentation results can be seen in Figure 6.

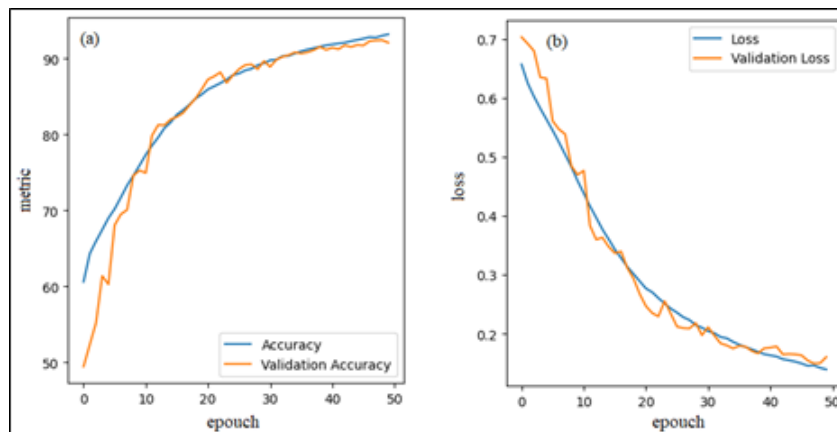


Figure 6. The Performance of DResNet on Graph (a) Accuracy (b) Loss

Based on Figure 6, it is found that the value of the accuracy and loss results using the segmentation results is said to be good. The training using the 50 epochs that were carried out shows that the accuracy and loss graphs obtained continue to improve. The results of the COVID prediction with the testing results show that 92 images were classified correctly, and 10 were classified incorrectly. The results of normal predictions with the results of testing show that 79 images were classified correctly, and 24 were classified incorrectly. The results of the pneumonia prediction with the testing results showed that 85 images were classified correctly, and 13 were classified incorrectly. Other results of the classification of segmentation results are 91% accuracy, an average precision value for each class is 86%, an average recall value for each class is 85%, and an average F1-Score value for each class is 84%. In addition to obtaining accuracy, precision, recall, and F1-Score, a graph of accuracy and loss for classification using

segmentation results is also obtained. With the classification results obtained, the performance graph of the classification model within all classification limits is seen in the ROC graph, which can be seen in Figure 7.

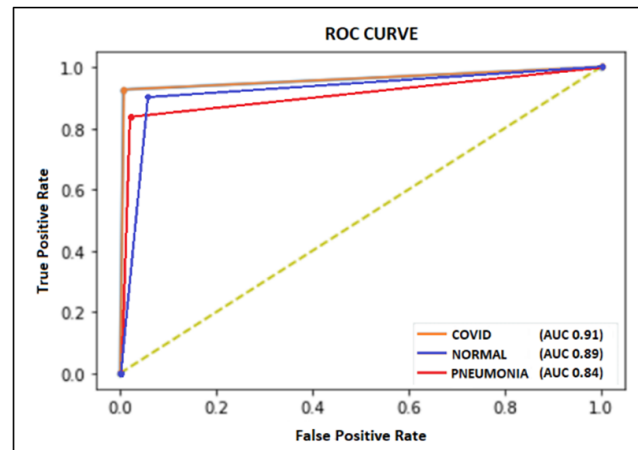


Figure 7. The Performance of Classification Results Using DResNet on The ROC Graph

Based on Figure 9, the resulting ROC value can be said to be good. The orange line indicates the area under the curve (AUC) for COVID-19, the blue line indicates the AUC for Normal, and the red line indicates the AUC for Pneumonia. The excellent classification results mean that machine learning of lung disease is working well. The results obtained from the classification will be compared with the results obtained using other methods by previous studies. The results of the classification evaluation carried out with DResNet were obtained compared to the results of other studies on COVID-19 and pneumonia. The results of this comparison can be seen in Table 4.

Table 4. Comparison of Classification Methods

Method	Results			
	Accuracy (%)	Precision (%)	Recalls (%)	F1-Score (%)
MobileNetV2 [29]	81	81.1	79.4	80.24
DenseNet-169 [18]	86	87	86	86
CNN and DeTraC [30]	95.12	97.91	-	-
Proposed Method	91	86	85	84

Based on Table 4, this research, in line with the research [29], obtained high accuracy, precision, and F1-Score above 80%, but this study did not use segmented images from lung segmentation and recalls below 80%. Recall and f1-score can show the model's positive prediction ratio. The research by [18] also shows high accuracy, precision, recalls, and F1-Score above 85%, but this study did not use segmented images from lung segmentation. The research by [30] also shows excellent accuracy and precision above 95%, but this study did not calculate recalls and F1-Score. The proposed method obtained excellent accuracy above 90%, high precision, recalls, and F1-Score above 84%. The performance results in classification are still not optimal, so further study can develop other architectures besides DResNet to obtain better classification performance results.

4. CONCLUSION

The novelty of this study is it combines segmentation and classification to determine lung disease with modified CNN architectures based on X-ray images. In the segmentation, a modified U-Net architecture with the addition of a dropout called DrU-Net is used. In the classification stage, the study proposed a modified ResNet architecture with the addition of a dropout called DResNet. Segmentation separates the lung organs from other organs in the X-ray image, but the classification is grouped under the Covid, Normal, and Pneumonia labels. The modification aims to simplify the complexity of the U-Net and Resnet architectures and prevent excessive parameter increases during training. The results of the segmentation performance of the DrU-Net architecture and classification using DResnet on the Convolutional Neural Network (CNN) architecture can be categorized as very good. The segmentation process using the DrU-net architecture works excellently and is robust based on the results of accuracy, precision, recall, F1-Score,

specificity, and IoU obtained above 90%. The performance results of accuracy, precision, recall, and F1-Score at the classification stage showed that the DResnet architecture works well in classifying lung disorders into three labels, namely Covid, Normal, and Pneumonia. However, the performance results of DResNet are still below 90%, so DResNet needs to be modified to obtain better results. The results of this study can be used as an alternative architecture for the segmentation and classification of other medical images.

5. ACKNOWLEDGEMENTS

This research can be completed thanks to the help of various parties. The author would like to thank the Rector of Universitas Sriwijaya and the Computation Laboratory of Mathematics and Natural Science Faculty for supporting this research.

6. DECLARATIONS

AUTHOR CONTRIBUTION

The first and the fourth authors helped revise the manuscript during the peer-review stage, and the second and the fifth authors conceived and designed works and collected data. The sixth author analyzed data and wrote an initial draft of the manuscript. The fourth author carried out a critical revision of the paper and final paper.

FUNDING STATEMENT

The research publication of this article was funded by DIPA of the Public Service Agency of Universitas Sriwijaya 2023. Nomor SP DIPA-023.17.2.6775151/2023, On November 30, 2022. By the Rector's Decree Number: 0188/UN9.3.1/SK/2023, on April 18, 2023.

COMPETING INTEREST

All authors have no competing interest to declare.

REFERENCES

- [1] Y. Qin, Y. Chen, J. Chen, K. Xu, F. Xu, and J. Shi, "The relationship between previous pulmonary tuberculosis and risk of lung cancer in the future," *Infectious Agents and Cancer*, vol. 17, no. 20, pp. 1–12, dec 2022.
- [2] T. Pranata, A. Desiani, B. Suprihatin, H. Hanum, and F. Efriliyanti, "Segmentation of the Lungs on X-Ray Thorax Images with the U-Net CNN Architecture," *Computer Engineering and Applications Journal*, vol. 11, no. 2, pp. 101–111, 2022.
- [3] A. M. Baig, A. Khaleeq, U. Ali, and H. Syeda, "Evidence of the COVID-19 Virus Targeting the CNS: Tissue Distribution, HostVirus Interaction, and Proposed Neurotropic Mechanisms," *ACS Chemical Neuroscience*, vol. 11, no. 7, pp. 995–998, apr 2020.
- [4] M. Abu-Farha, T. A. Thanaraj, M. G. Qaddoumi, A. Hashem, J. Abubaker, and F. Al-Mulla, "The Role of Lipid Metabolism in COVID-19 Virus Infection and as a Drug Target," *International Journal of Molecular Sciences*, vol. 21, no. 10, pp. 1–11, may 2020.
- [5] P. Pagliano, C. Sellitto, V. Conti, T. Ascione, and S. Esposito, "Characteristics of viral pneumonia in the COVID-19 era: an update," *Infection*, vol. 49, no. 4, pp. 607–616, 2021.
- [6] M. Nour, Z. Cömert, and K. Polat, "A Novel Medical Diagnosis model for COVID-19 infection detection based on Deep Features and Bayesian Optimization," *Applied Soft Computing*, vol. 97, no. December, pp. 1–13, dec 2020.
- [7] M. Yahyatabar, P. Jouviet, and F. Cheriet, "Dense-Unet: a light model for lung fields segmentation in Chest X-Ray images," in *2020 42nd Annual International Conference of the IEEE Engineering in Medicine & Biology Society (EMBC)*, 2020, pp. 1242–1245.
- [8] H. Shaziya and K. Shyamala, "Pulmonary CT Images Segmentation using CNN and UNet Models of Deep Learning," in *2020 IEEE Pune Section International Conference, PuneCon 2020*, 2020, pp. 195–201.

- [9] X. Zhang, J. Zhou, W. Sun, and S. K. Jha, "A Lightweight CNN Based on Transfer Learning for COVID-19 Diagnosis," *Computers, Materials and Continua*, vol. 72, no. 1, pp. 1123–1137, 2022.
- [10] M. F. Aslan, K. Sabanci, A. Durdu, and M. F. Unlarsen, "COVID-19 diagnosis using state-of-the-art CNN architecture features and Bayesian Optimization," *Computers in Biology and Medicine*, vol. 142, no. March, pp. 1–11, mar 2022.
- [11] A. Das, "Adaptive UNet-based Lung Segmentation and Ensemble Learning with CNN-based Deep Features for Automated COVID-19 Diagnosis," *Multimedia Tools and Applications*, vol. 81, no. 4, pp. 5407–5441, 2022.
- [12] M. F. Aslan, "A robust semantic lung segmentation study for CNN-based COVID-19 diagnosis," *Chemometrics and Intelligent Laboratory Systems*, vol. 231, no. 15, pp. 1–12, dec 2022.
- [13] S. Niranjana Kumar, P. M. Bruntha, S. Isaac Daniel, J. A. Kirubakar, R. Elaine Kiruba, S. Sam, and S. Immanuel Alex Pandian, "Lung Nodule Segmentation Using UNet," in *2021 7th International Conference on Advanced Computing and Communication Systems (ICACCS)*, vol. 1, 2021, pp. 420–424.
- [14] S. A. Khan, M. Nazir, M. A. Khan, T. Saba, K. Javed, A. Rehman, T. Akram, and M. Awais, "Lungs nodule detection framework from computed tomography images using support vector machine," *Microscopy Research and Technique*, vol. 82, no. 8, pp. 1256–1266, aug 2019.
- [15] D. Sarwinda, R. H. Paradisa, A. Bustamam, and P. Anggia, "Deep Learning in Image Classification using Residual Network (ResNet) Variants for Detection of Colorectal Cancer," *Procedia Computer Science*, vol. 179, pp. 423–431, 2021.
- [16] B. Li and D. Lima, "Facial expression recognition via ResNet-50," *International Journal of Cognitive Computing in Engineering*, vol. 2, no. June, pp. 57–64, jun 2021.
- [17] S. Bharati, P. Podder, M. R. H. Mondal, and V. S. Prasath, "CO-ResNet: Optimized ResNet model for COVID-19 diagnosis from X-ray images," *International Journal of Hybrid Intelligent Systems*, vol. 17, no. 1-2, pp. 71–85, jul 2021.
- [18] T. A. Youssef, B. Aissam, D. Khalid, B. Imane, and J. E. Miloud, "Classification of chest pneumonia from x-ray images using new architecture based on ResNet," in *2020 IEEE 2nd International Conference on Electronics, Control, Optimization and Computer Science (ICECOCS)*, 2020, pp. 1–5.
- [19] Y. Ma, X. Xu, and Y. Li, "LungRN+NL: An Improved Adventitious Lung Sound Classification Using Non-Local Block ResNet Neural Network with Mixup Data Augmentation," in *Interspeech 2020*. ISCA: ISCA, oct 2020, pp. 2902–2906.
- [20] A. Desiani, Erwin, B. Suprihatin, F. Efriliyanti, M. Arhami, and E. Setyaningsih, "VG-DropDNet a Robust Architecture for Blood Vessels Segmentation on Retinal Image," *IEEE Access*, vol. 10, no. June, pp. 92 067–92 083, 2022.
- [21] J. Li, Y. Zhang, L. Gao, and X. Li, "Arrhythmia Classification Using Biased Dropout and Morphology-Rhythm Feature With Incremental Broad Learning," *IEEE Access*, vol. 9, pp. 66 132–66 140, 2021.
- [22] A. A. A. Ali and S. Mallaiah, "Intelligent handwritten recognition using hybrid CNN architectures based-SVM classifier with dropout," *Journal of King Saud University - Computer and Information Sciences*, vol. 34, no. 6, pp. 3294–3300, 2022.
- [23] D. Milanés-Hermosilla, R. Trujillo Codorniú, R. López-Baracaldo, R. Sagaró-Zamora, D. Delisle-Rodriguez, J. J. Villarejo-Mayor, and J. R. Núñez-Álvarez, "Monte Carlo Dropout for Uncertainty Estimation and Motor Imagery Classification," *Sensors*, vol. 21, no. October, pp. 1–18, oct 2021.
- [24] C. Guo, M. Szemenyei, Y. Yi, W. Wang, B. Chen, and C. Fan, "SA-UNet: Spatial Attention U-Net for Retinal Vessel Segmentation," in *2020 25th International Conference on Pattern Recognition (ICPR)*, 2021, pp. 1236–1242.
- [25] Faiz Nashrullah, Suryo Adhi Wibowo, and Gelar Budiman, "The Investigation of Epoch Parameters in ResNet-50 Architecture for Pornographic Classification," *Journal of Computer, Electronic, and Telecommunication*, vol. 1, no. 1, pp. 1–8, 2020.
- [26] X. Wang, X. Deng, Q. Fu, Q. Zhou, J. Feng, H. Ma, W. Liu, and C. Zheng, "A Weakly-Supervised Framework for COVID-19 Classification and Lesion Localization from Chest CT," *IEEE Transactions on Medical Imaging*, vol. 39, no. 8, pp. 2615–2625, aug 2020.

-
- [27] N. Paluru, A. Dayal, H. B. Jenssen, T. Sakinis, L. R. Cenkeramaddi, J. Prakash, and P. K. Yalavarthy, "Anam-Net: Anamorphic Depth Embedding-Based Lightweight CNN for Segmentation of Anomalies in COVID-19 Chest CT Images," *IEEE Transactions on Neural Networks and Learning Systems*, vol. 32, no. 3, pp. 932–946, mar 2021.
- [28] G. Pezzano, O. Díaz, V. Ribas, and P. Radeva, "CoLe-CNN+: Context learning - Convolutional neural Network for COVID-19-Ground-Glass-Opacities detection and segmentation," *Computers in Biology and Medicine*, vol. 136, no. 104689, pp. 1–10, 2021.
- [29] A. Soud, N. Sakli, and H. Sakli, "Classification and Predictions of Lung Diseases from Chest X-rays Using MobileNet V2," *Applied Sciences*, vol. 11, no. 6, pp. 1–16, mar 2021.
- [30] A. Abbas, M. M. Abdelsamea, and M. M. Gaber, "Classification of COVID-19 in chest X-ray images using DeTraC deep convolutional neural network," *Applied Intelligence*, vol. 51, no. 2, pp. 854–864, feb 2021.